

SCIENTIFIC COMMUNICATIONS

INVISIBLE GOLD AT ZARSHURAN, IRAN

H. H. ASADI,

*Ministry of Culture and Higher Education, Dr. Beheshti Avenue, Shahid Sabounchi Cross, Tehran, Iran, and
International Institute of Aerospace Survey and Earth Sciences, Kanaalweg 3, 2628 EB Delft, Netherlands*

J. H. L. VONCKEN,[†]

Delft University of Technology, Subfaculty of Applied Earth Sciences, Mijnbouwstraat 120, 2628 RX Delft, Netherlands

AND M. HALE

*International Institute of Aerospace Survey and Earth Sciences, Kanaalweg 3, 2628 EB Delft, Netherlands, and
Delft University of Technology, Subfaculty of Applied Earth Sciences, Mijnbouwstraat 120, 2628 RX Delft, Netherlands*

Abstract

Although micron-size particles of metallic gold are observed at the Zarshuran gold deposit, northwest Iran, the quantities do not account for the gold concentrations determined by chemical analyses. The presence of invisible gold has been established by means of trace element electron microprobe analyses of pyrite, arsenian pyrite, orpiment, realgar, stibnite, getchellite, sphalerite, and lead sulfosalts. Quantitative point analyses indicate that invisible gold is present in anhedral pyrite, arsenian pyrite overgrowth rims on gold- and arsenic-free euhedral pyrite, in massive, network, and colloform arsenian pyrite, and in massive and colloform sphalerite intimately intergrown with colloform arsenian pyrite. Gold in these forms adequately explains the measured gold concentrations at Zarshuran. The invisible gold owes its origin to solid-solution deposition and/or encapsulation of submicron-size particles of metallic gold.

Introduction

At Zarshuran, north of Takab in northwest Iran (Fig. 1), disseminated gold occurs in Precambrian sedimentary rocks. Recent exploration for gold has established a probable reserve of 2.5 million tons (Mt) of ore with an average grade of 10 g/t gold (Samimi, 1992).

The Precambrian stratigraphy of the Zarshuran area consists of, from oldest to youngest, a basement of schist, the Chaldagh unit (limestone), and the Zarshuran unit (carbonaceous black shale with silica and carbonate intercalations). Gold is in hydrothermal veins of massive quartz (jasperoid) and quartz veinlets formed by carbonate replacement along high-angle faults. The faults trend east-west and northwest-southeast in the Chaldagh limestone. Gold also occurs as disseminations in the carbonaceous, siliceous, and calcareous beds within the Zarshuran black shale. The Chaldagh limestone is mineralized at its contacts with the schist and with the Zarshuran unit. In close spatial association with the mineralized Precambrian rocks is a highly altered Oligocene-Miocene granitoid stock, which itself is weakly mineralized.

Quartz, calcite, dolomite, and clays are the principal minerals of the host rocks. Decalcification, silicification, and argillization characterize mineralized rocks. Decalcification increased the porosity and permeability of the host rocks and thus provided favorable sites for hydrothermal mineralization. The ore consists mainly of orpiment and pyrite, and to a lesser extent sphalerite, galena, realgar, and stibnite, with

subordinate cinnabar (HgS), lorandite (TlAsS₂), christite (TlHgAsS₃), coloradoite (HgTe), getchellite (AsSbS₃), ak-tashite (Cu₆Hg₃As₄S₁₂), baumhuerite (Pb₃As₄S₉), boulang-gerite (Pb₅Sb₄S₁₁), geochronite (Pb₁₄(Sb, As)₆S₂₃), pligionite (Pb₅Sb₃S₁₁), and twinnite (Pb(Sb, As)₂S₄; Asadi et al., 1999). Sulfide oxidation is mainly confined to veins, veinlets, and fracture zones. Quartz, calcite, fluorite, hematite, and barite are the main gangue minerals. Accessory minerals include apatite (Ca₅(PO₄)₃(OH, F, Cl)), rutile (TiO₂), zircon (ZrSiO₂), and xenotime (YPO₄). There are no gold minerals except for rare native gold, which is present in quantities insufficient to explain the gold grade established by exploration trenches, boreholes, and tunnels.

Many characteristics of the Zarshuran deposit are similar to other disseminated gold deposits hosted by sedimentary rocks. In those of the western United States, gold is rarely visible but occurs invisibly in a number of mineral phases (Bakken et al., 1991; Arehart et al., 1993). In order to determine if similar invisible gold occurs at Zarshuran, trace element analyses of 15 mineralized samples from outcrops, trenches, boreholes, and tunnels were carried out by electron microprobe analysis. Bulk chemical analyses for ore and ore-related trace elements were performed on corresponding subsamples.

Methods

Trace levels of gold in other minerals can be determined by electron microprobe analysis provided the X-ray intensity of the microprobe is maximized and the peak to background

[†] Corresponding author: email, J.H.L.Voncken@ta.tudelft.nl

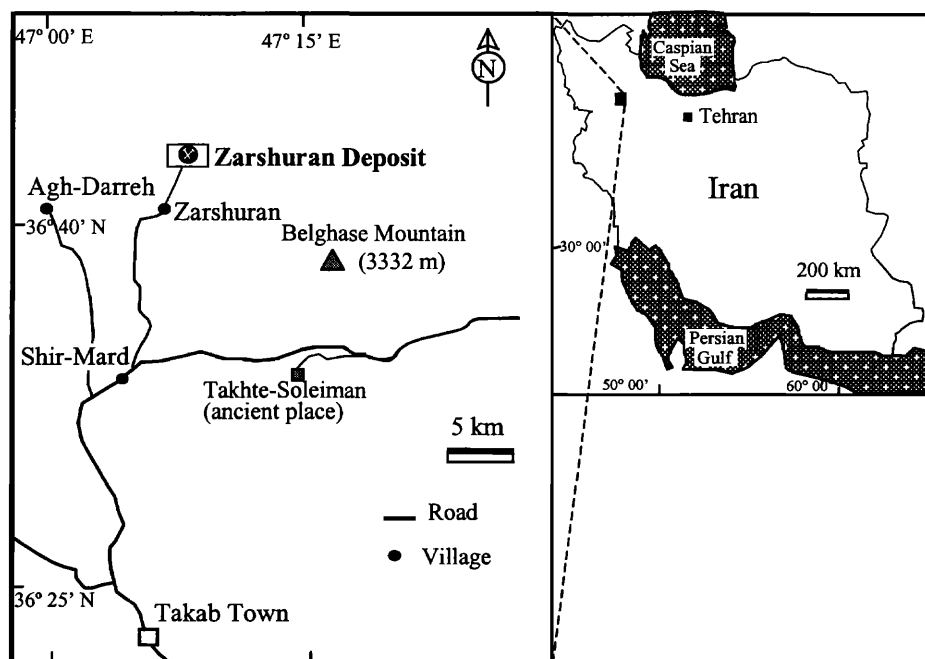


FIG. 1. Sketch map of Iran showing location of Zarshuran gold deposit.

ratio for the X-ray line under consideration is optimized. These operating characteristics require maximum achievable accelerating voltage, highest possible beam current, and long counting times (Graham et al., 1989; Cook and Chryssoulis, 1990; Robinson and Graham, 1992; Johansen and Kojonen, 1996; Gervilla et al., 1997; Kojonen and Johansen, 1997).

Electron microprobe analyses of the Zarshuran samples were performed with a JEOL 8800 at the Subfaculty of Applied Earth Sciences, Delft University of Technology. The analytical conditions were (1) 40 kV accelerating voltage, (2) 3.8×10^{-8} A beam current, (3) X-ray line of Au-L α on the LIF crystal, (4) counting times of 300 s on peak and background, and (5) native gold as the analytical standard. Measurements were carried out first on the peak and subsequently on the upper and lower background positions. The applied alternating peak and background measurements required special software which was available for our instrument. However, it was found that the instrument was fairly stable under these conditions, so that errors due to drift were minimal. The detection limit for gold is 20 ppm according to the calculation made by the instrument software, i.e., $D.L. = 3/nc \cdot \sqrt{2 \cdot IB/tB} \cdot wt$, where D.L. = detection limit, nc = net count (cps) of the standard specimen, IB = mean background intensity (cps) of unknown specimen, tB = measurement time (s) at background position, and wt = weight percent of standard specimen. The detection limit calculated according to the Zieboldt equation (Zieboldt, 1967) is slightly lower. In similar work, Johansen and Kojonen (1996) reported a detection limit of 15 ppm gold.

The 15 samples studied by electron microprobe analysis were also analyzed for Au, As, Ag, Sb, Hg, Tl, Te, Zn, S, and C by atomic absorption spectrophotometry (AAS) at the Geological Laboratory in Teplice, Slovakia. These data were used primarily to support the electron microprobe analyses results. These AAS results were merged with the AAS results

from 838 borehole samples and 47 other representative mineralized and unmineralized rock samples from outcrops, trenches, and tunnels at Zarshuran to create a geochemical database of 900 samples. This database was used to prepare bar charts showing the ranges of gold concentrations in different rock types and to identify correlations between gold and other elements.

Results

Arsenian pyrite occurs as overgrowths on large euhedral pyrite crystals. A later network and massive arsenian pyrite encloses the overgrowth rims. The latest generation of arsenian pyrite is colloform in texture and intimately intergrown with massive and colloform sphalerite.

Occurrence of visible gold

Karimi (1992) reported the occurrence of micron-size gold in the silicified ores. Nevertheless, examination by high-resolution optical microscopy and electron analyses of several silicified ore samples, including those found by chemical analyses to have the highest gold concentrations, failed to reveal any native gold associated with silica. Sparse gold was found only in close association with an arsenic-mercury-thallium sulfide, both occurring as inclusions in a matrix of microcrystalline orpiment. These inclusions were first observed by optical microscopy and subsequently confirmed by electron microprobe analysis (Fig. 2). Qualitative microprobe analysis of a gold grain gave no indication of the presence of other metals commonly found with gold (e.g., Ag, Te, Se).

Gold concentrations and associations

Gold at Zarshuran is hosted mainly by the jasperoid, silicified shale, and silicified limestone (Fig. 3). Within these rock types, high gold concentrations tend to be found in samples that contain visible pyrite and orpiment.

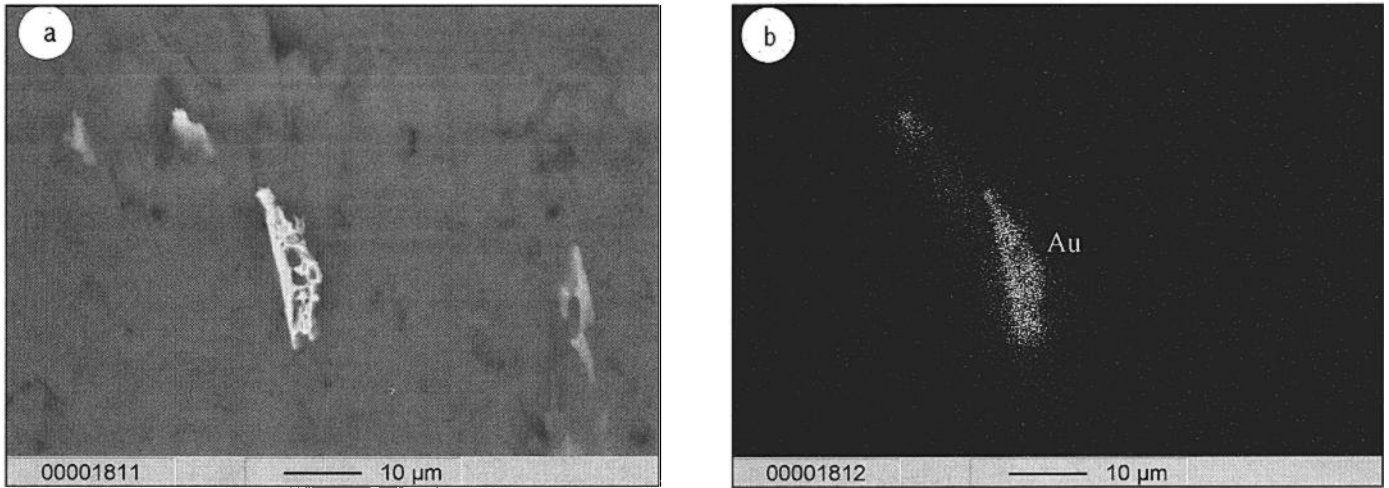


FIG. 2. Scarce native gold at Zarshuran. (a). Back-scattered electron microprobe image of dendritic gold grain in microcrystalline orpiment matrix. (b). Corresponding X-ray image showing Au concentration.

Gold shows strong positive correlations with arsenic and mercury, and weaker positive correlations with antimony and zinc (Fig. 4). It has no significant correlation with other elements. Arsenic has a very strong positive correlation with mercury and antimony and a weaker positive correlation with zinc.

Among the samples examined by electron microprobe analyses, bulk gold contents determined by AAS ranged from 0.08 to 26.53 ppm. The highest gold concentrations were found in samples containing visible pyrite, orpiment, and sphalerite (Table 1).

Occurrence of invisible gold

The scarcity of visible gold, coupled with the high concentrations of gold in the mineralized rocks at Zarshuran, lends credence to the occurrence of invisible gold. The positive correlations between gold and arsenic, mercury, antimony, and zinc guided the search for this gold to the arsenic, mercury, antimony, and zinc sulfides (orpiment, realgar, arsenian pyrite, cinnabar, stibnite, and sphalerite). Where applicable, a distinction was made between different textures (and, therefore, possibly different generations) of the same mineral. The

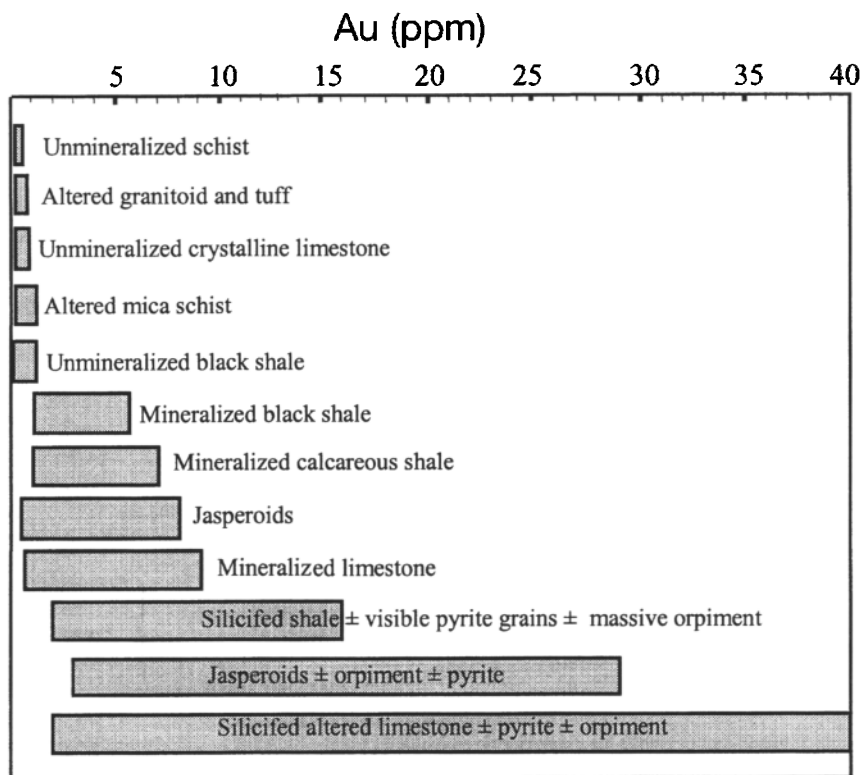


FIG. 3. Distribution of gold in different rock types at Zarshuran, based on analyses of 900 samples by AAS.

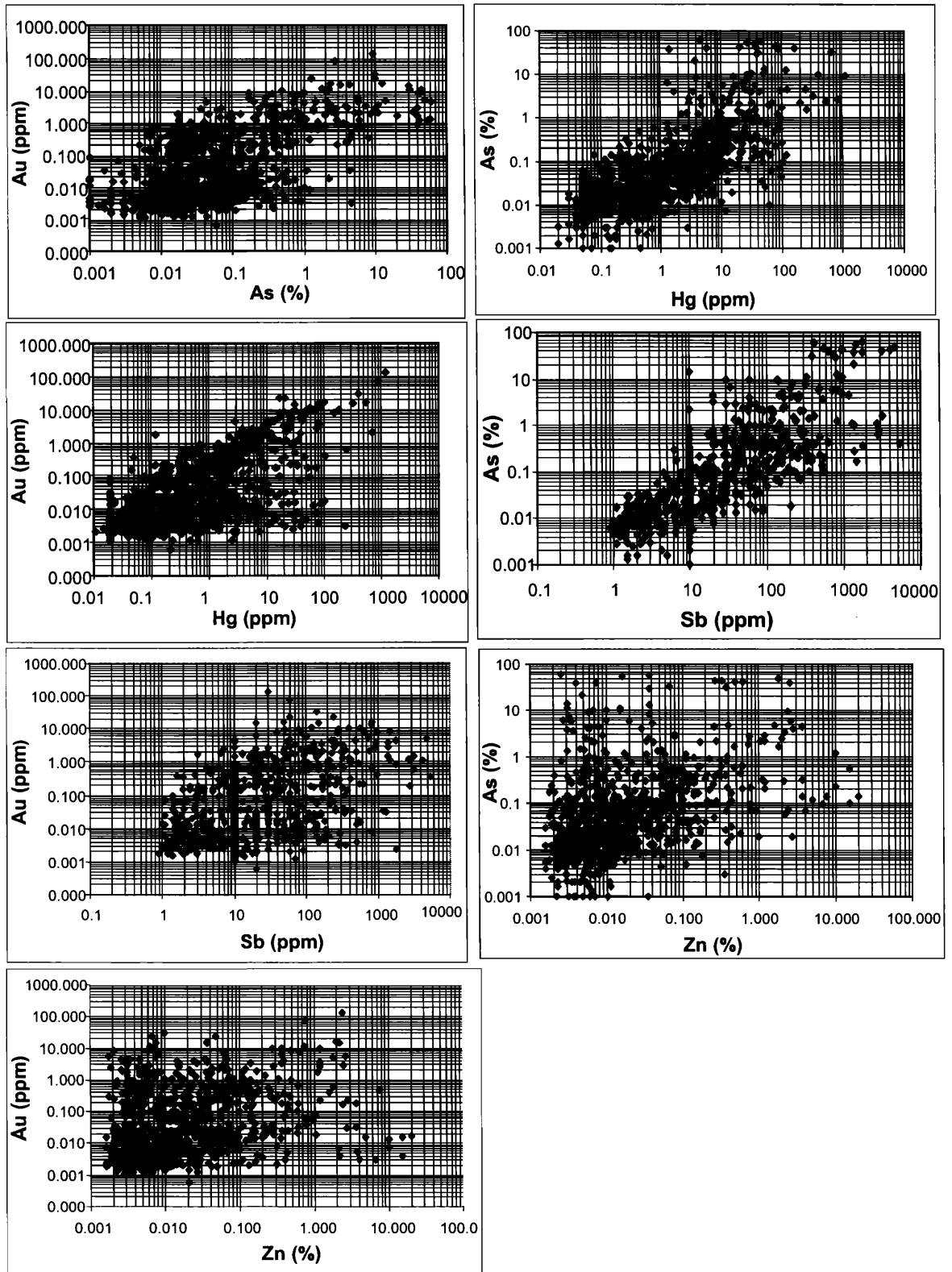


FIG. 4. Scatter diagrams (logarithmic axes) for Au-As, Au-Hg, Au-Sb, Au-Zn, As-Hg, As-Sb, and As-Zn at Zarshuran, based on analyses of 900 samples by AAS.

TABLE 1. Bulk Chemical Analyses of 15 Samples (in ppm, except as stated)

Description	Sample	Au	Ag	As (%)	Sb (%)	Tl	Hg	Te	Zn (%)	S (%)
Unmineralized rocks										
Schist	15486	0.08	<0.2	0.05	0.002	0.5	0.64	<0.5	0.041	1.00
Andesite	15483	0.10	<0.2	0.02	0.013	4.5	4.89	<0.5	0.101	0.72
Altered granitoid	15485	0.14	0.2	0.04	0.003	1.4	3.06	<0.5	0.064	0.63
Dense limestone	15487	0.18	0.2	0.05	0.002	5.7	1.46	<0.5	0.067	2.77
Altered limestone	15491	0.16	<0.2	0.25	0.002	1.3	4.45	<0.5	0.272	0.46
Weakly silicified limestone	15493	0.36	0.2	0.12	0.032	1.6	4.53	1.0	0.100	0.61
Mineralized rocks										
Black shale	15488	0.18	5.8	0.22	0.040	8.8	14.66	1.8	0.960	9.09
Black shale	15492	9.57	0.4	0.06	0.007	20.5	26.14	<0.5	0.055	1.91
Black shale + getchellite + py	15489	15.24	2.2	3.14	3.100	360.0	606.6	9.0	4.818	10.00
Jasperoid	15494	0.64	10.0	18.00	0.70	50.0	43.8	55.3	0.780	13.51
Jasperoid + sph + fl	15484	0.58	210.4	0.47	0.750	12.6	499.3	5.7	30.813	19.74
Jasperoid + barite	15481	2.42	3.2	3.22	0.029	8.0	62.60	18.1	0.103	4.90
Jasperoid + py + sph	15482	10.75	17.2	1.05	0.627	185.0	142.2	18.2	23.625	25.05
Jasperoid + py + orp	15490	26.53	10.0	16.85	1.940	14.9	327.7	125.0	0.410	11.91
Massive orpiment and realgar	15480	0.14	1.2	58.50	2.250	1.6	8.78	316.0	NA	38.58

Abbreviations: fl = fluorite; orp = orpiment; py = pyrite; sph = sphalerite; NA = not analyzed

Detection limits: Ag = 0.2 ppm, Te = 0.5 ppm; analytical method = atomic absorption spectrophotometry (AAS)

search was also extended to pyrite and lead sulfosalts, such as getchellite. The results of electron microprobe analyses of these minerals for trace gold are summarized in Table 2.

After orpiment, pyrite and arsenian pyrite are the most abundant sulfide minerals at Zarshuran. Euhedral to subhedral pyrite commonly occurs as fine-grained crystals in quartz and occasionally in fluorite, barite, calcite, and sphalerite. In this variety of pyrite, gold and, in most cases, arsenic were found to be below detection limit.

Anhedral pyrite grains commonly occur in an orpiment matrix, and electron microprobe analysis revealed that this variety of pyrite contains 40 to 100 ppm gold, an average of 0.19 percent arsenic, and up to 2.4 percent arsenic. Where arsenic concentrations exceed 1 percent, this pyrite can be considered to be arsenian pyrite. The gold concentration in this type of pyrite displays a positive correlation with the arsenic concentration. Owing to the combination of its relative abundance and typically high gold content, arsenian pyrite is the most

TABLE 2. Range of Concentrations of Gold, Arsenic, and Mercury in Sulfide and Sulfosalt Minerals in 15 Samples Examined by Electron Microprobe Analysis

Mineral / phase	No. analyses	Au (ppm)	As (%)	Hg (ppm)	Observations
Orpiment	15	<20		<250–710	Rare (sub)micron-size grains of metallic gold
Realgar	7	<20		<250–660	
Stibnite, getchellite and Pb sulfosalts	10	<20			
Euhedral pyrite	5	<20	<0.04, 0.22	<250	Core of pyrite with overgrowth rims, quartz matrix; one analysis only 0.22% As
Anhedral pyrite	10	40–100	0.04–2.4	<250	Occurs in orpiment matrix
Overgrowth, network and massive arsenian pyrite	8	<20–140	1.08–3.4	<250–400	Overgrowths on euhedral pyrite, network and massive varieties adjacent; quartz matrix; Au, As and Hg content variable
Colloform arsenian pyrite (melnicovite)	10	1,060–1,300	3.16–4.73	4,420–5,940	Late-stage mineral occurring in quartz and sometimes intimately intergrown with massive and colloform sphalerite
Colloform and massive sphalerite	10	110–390	<0.04–0.65	<250–1,970	Iron-rich colloform and massive sphalerite intimately intergrown with colloform pyrite; Au content correlates with Fe content

Detection limits: Au = 20 ppm, Hg = 250 ppm, and As = 0.045 percent

important gold-bearing mineral at Zarshuran. Three types of arsenian pyrite are recognized.

The earliest gold-bearing arsenian pyrite is very abundant in association with sphalerite, euhedral pyrite, and lead sulfosalts (mainly geochronite and baumhauerite) in quartz. This arsenian pyrite occurs as overgrowths on some large (5–300 μm) euhedral pyrite crystals. These overgrowth rims, identified by high-resolution optical microscopy (1,000 \times magnification, oil immersion lens) and confirmed by microprobe analysis, vary in thickness from 1 to 20 μm . Geochronite and baumhauerite occasionally enclose the overgrowth rims (Fig. 5). Electron microprobe analyses of these rims pinpoint high arsenic concentrations (1.08–1.65%), high mercury concentrations (<250–480 ppm), and gold concentrations of up to 140 ppm. These concentrations compare with low arsenic (<0.04%, one analysis = 0.22%) and gold and mercury concentrations below the 20 and 350 ppm detection limits, respectively, in the euhedral pyrite core. Within the rim, the

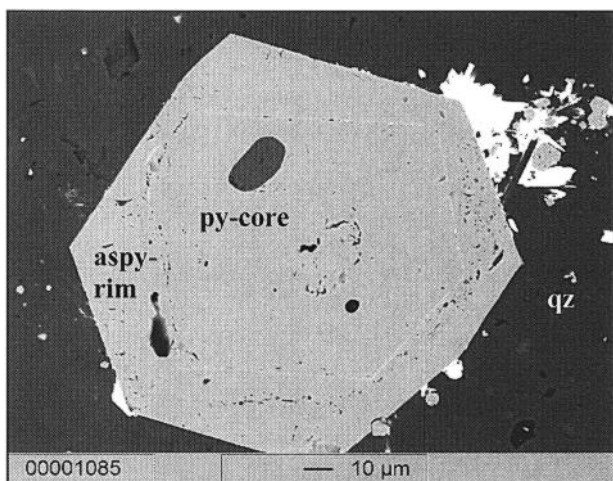


FIG. 5. Back-scattered electron microphotograph of overgrowth rim (aspy-rim) of Au-bearing arsenian pyrite on preexisting barren pyrite (py-core); bright masses on the outer margin of the arsenian pyrite rim are geochronite and baumhauerite.

highest arsenic and gold concentrations were detected by electron microprobe analyses at the boundary of the overgrowth rims with the euhedral pyrite core. This boundary exhibits a brighter color than the rest of the rims in the back-scattered electron microphotograph.

A second type of arsenian pyrite encloses the overgrowth rim and, due to its high arsenic and mercury contents (up to 3.4% and 5,940 ppm, respectively), appears bright in a back-scattered electron microphotograph. This type of arsenian pyrite shows a network and massive texture attributed to its precipitation from hydrothermal solutions percolating through microfractures in quartz (Fig. 6). It is occasionally intergrown with massive sphalerite in quartz. Microprobe analyses show an average higher gold concentration in this type of arsenian pyrite (116 ppm) compared to overgrowth rims (90 ppm).

A third type of arsenian pyrite exhibits a colloform texture. Colloform arsenian pyrite, or melnicovite, contains 1,030 to 1,300 ppm gold and up to 4.73 percent arsenic. The highest concentrations of gold, arsenic, and mercury tend to be found in the rim (Fig. 7, Table 2). Melnicovite occurs in the hydrothermal silica matrix and commonly is intimately intergrown with massive and colloform sphalerite.

Sphalerite, the most abundant sulfide after orpiment, pyrite, and arsenian pyrite, is present as individual anhedral grains associated with galena and also as massive and colloform sphalerite intergrown with massive arsenian pyrite and melnicovite (Fig. 8). Gold was detected in massive and colloform sphalerite in concentrations from 110 to 390 ppm. The highest gold values are found in massive and colloform sphalerite that also contains elevated arsenic and mercury concentrations. A sample of jasperoid with anhedral sphalerite and fluorite (sample 15484) was found by AAS to contain 0.58 ppm gold and 0.47 percent arsenic, whereas a sample of jasperoid with massive sphalerite and pyrite (sample 15482) was found to contain 10.75 ppm gold and 1.05 percent arsenic (Table 1).

Orpiment and realgar are very abundant at Zarshuran and constitute an arsenic ore that currently is worked on a small scale. These minerals mainly occur as massive grains associated with jasperoid and carbonate minerals. Whereas electron

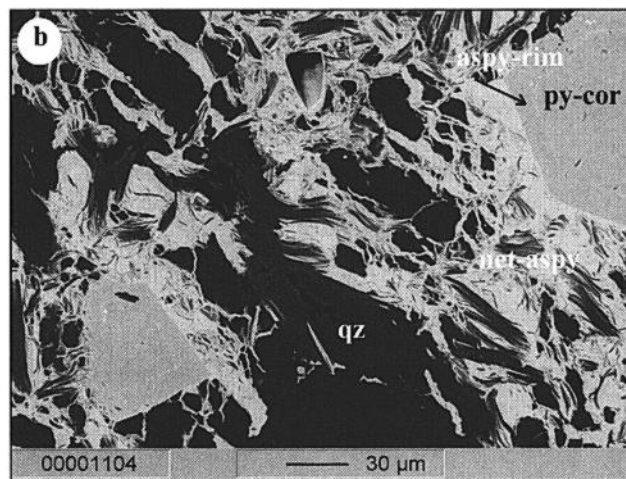
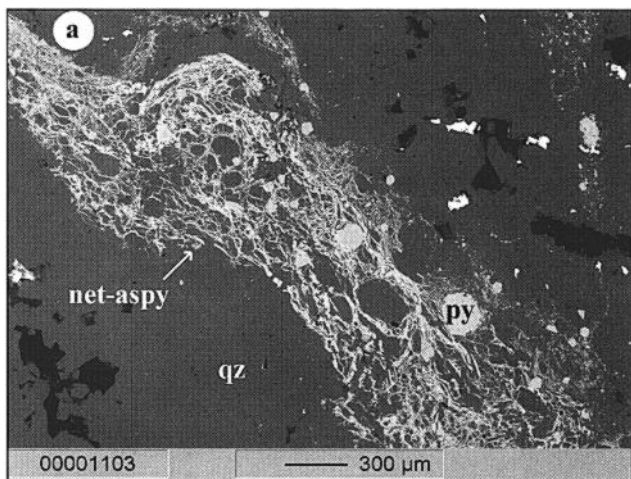


FIG. 6. Back-scattered electron microphotographs of network arsenian pyrite (net-aspy) in quartz matrix. (a). Overview. (b). Detail showing the bright net-aspy surrounding rimmed pyrite (py).

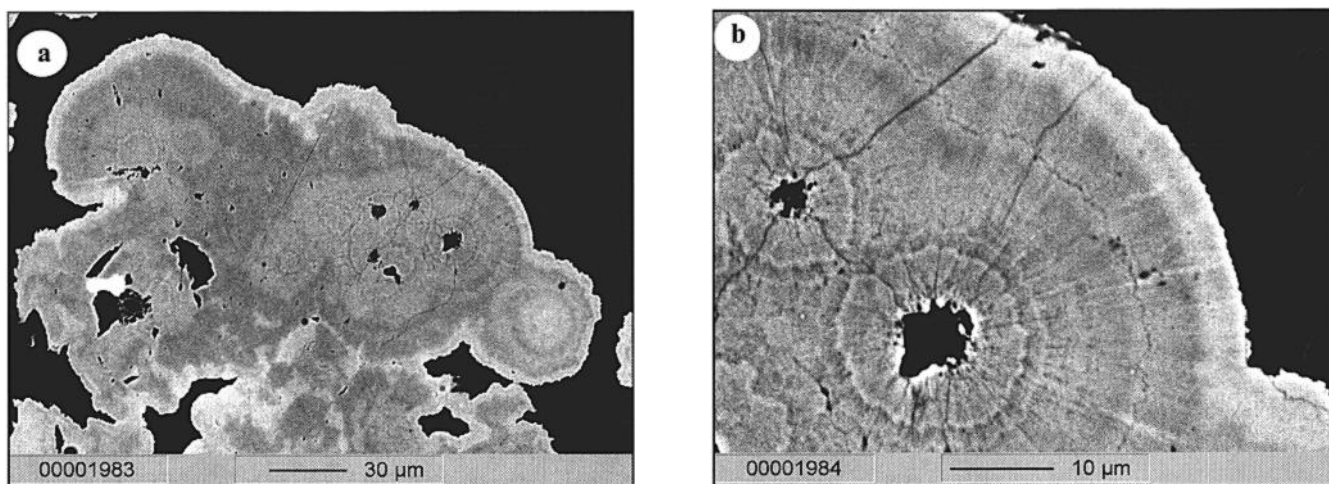


FIG. 7. Back-scattered electron microphotographs of colloform arsenian pyrite (melnicovite). (a). Overview. (b). Detail showing bright rims rich in arsenic and with higher gold concentration.

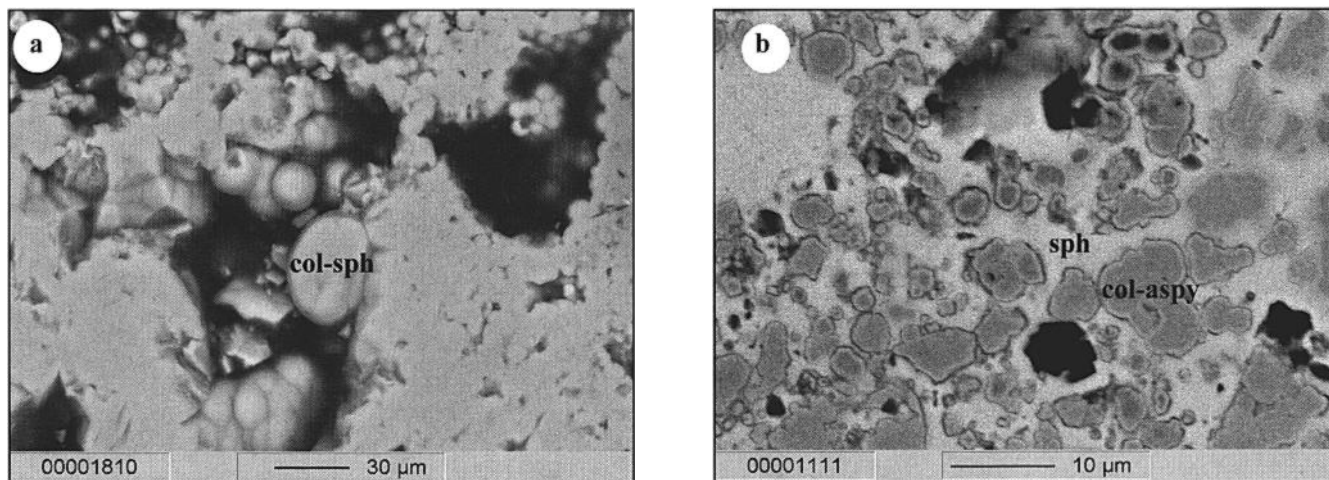


FIG. 8. Back-scattered electron microphotographs of sphalerite. (a). Colloform sphalerite (col-sph). (b). Massive sphalerite (sph, light gray) intimately intergrown with colloform arsenian pyrite (col-asp, dark gray).

microprobe analyses of orpiment and realgar did not reveal any gold concentration above the 20 ppm detection limit, bulk chemical analyses of dense microcrystalline orpiment occasionally yielded high gold concentrations up to 158 ppm, presumably due to the presence of rare native gold and of gold-bearing pyrite in orpiment.

Discussion

Gold in rocks altered to hydrothermal silica at Zarshuran is incorporated mainly into arsenian pyrite. By electron microprobe analyses this gold is traced to three sites: (1) the arsenian pyrite overgrowth rims on euhedral pyrite, (2) the network and massive arsenian pyrite associated with such overgrowth rims, and (3) colloform arsenian pyrite. On a microscale, gold concentrations increase from a barren euhedral pyritic core into an arsenian pyrite rim, and then further increase into the surrounding network, massive, and colloform arsenian pyrite. The occurrence of a gold-rich periphery on

barren pyrite has been noted at sediment-hosted disseminated gold deposits in Nevada. Radtke et al. (1972) and Wells and Mullens (1973) reported gold on the surfaces of pyrite at Carlin, and Radtke (1985) found enrichments of arsenic, mercury, antimony, and gold on the rims of some of the large pyrite grains at both Carlin and Cortez. Similarly, mercury at Zarshuran is concentrated with gold in the arsenian pyrite overgrowth rims. From their examination of five sediment-hosted disseminated gold deposits in Nevada, Arehart et al. (1993) suggested that gold was deposited with arsenic as coupled solid solution in arsenian pyrite. Comparable associations at Zarshuran suggest that this also may be the principal mechanism of gold deposition there.

Orpiment is the most abundant sulfide at Zarshuran and is an important gold carrier. Although Dickson et al. (1975) found that synthetic orpiment and realgar may contain 200 ppm gold as submicron-size particles and up to 2,000 ppm gold as solid solution, electron microprobe analyses of

Zarshuran orpiment and realgar revealed less than 20 ppm gold in these minerals. Rather, gold is attributed to scarce micron-sized native gold and gold-bearing anhedral pyrite in the orpiment matrix. At the sediment-hosted disseminated gold deposit at Carlin, Nevada, Bakken et al. (1989) noted submicron-size gold in pyrite and cinnabar.

Radtke et al. (1972) and Wells and Mullens (1973) reported gold in sphalerite at Carlin. At Zarshuran, almost all massive and colloform sphalerite studied by electron microprobe analysis showed a significant quantity of gold. The zoned texture and chemical variations of the colloform sphalerite suggest that layers of sphalerite alternate with layers of melnicovite. Thus, the gold-hosting role of this sphalerite may owe much to its intimate association with melnicovite, the host for the highest concentrations of gold at Zarshuran.

Conclusions

Invisible gold at Zarshuran occurs in melnicovite (up to 1,300 ppm), arsenian pyrite (up to 140 ppm), massive and colloform sphalerite (up to 390 ppm) associated with hydrothermal silica, and in anhedral pyrite (up to 100 ppm) in the orpiment matrix. Micron-size visible gold, found in inclusions in microcrystalline orpiment, makes an insignificant contribution to the total gold concentration. Several of the modes of occurrence of gold at Zarshuran have been recorded previously in sediment-hosted disseminated gold deposits in Nevada. It seems appropriate, therefore, to classify Zarshuran as a sediment-hosted disseminated gold deposit.

Acknowledgments

We would like to thank Radko Kuhnel and P. Sulousky for the confirmatory microprobe analyses of gold in sphalerite at the laboratory of the Department of Mineralogy, Masaryk University, Brno, Czech Republic.

August 27, 1998; June 4, 1999

REFERENCES

- Arehart, G.B., Chryssoulis, S.L., and Kesler, S.E., 1993, Gold and arsenic in iron sulfides from sediment-hosted disseminated gold deposits: Implications for depositional processes: *ECONOMIC GEOLOGY*, v. 88, p. 171–185.
- Asadi, H.H., Voncken, J.H.L., Kuhnel, R.A., and Hale, M., 1999, Petrology, mineralogy and geochemistry of the Zarshuran Carlin-like gold deposit: *Mineralium Deposita*, in press.
- Bakken, B.M., Hochella, M.F., Marshall, A.F., and Turner, A.M., 1989, High-resolution microscopy of gold in unoxidized ore from the Carlin mine, Nevada: *ECONOMIC GEOLOGY*, v. 84, p. 171–179.
- Bakken, B.M., Brigham, R.H., and Fleming, A.F., 1991, The distribution of gold in unoxidized ore from Carlin-type deposits revealed by secondary ion mass spectrometry (SIMS) [abs.]: *Geological Society of America Annual Meeting, Abstracts*, v. 52, p. 228.
- Cook, N.J., and Chryssoulis, S.L., 1990, Concentrations of invisible gold in common sulfides: *Canadian Mineralogist*, v. 28, p. 1–16.
- Dickson, F.W., Radtke, A.S., Weissberg, B.G., and Heropoulos, C., 1975, Solid solutions of antimony, arsenic, and gold in stibnite (Sb_2S_3), orpiment (As_2S_3), and realgar (As_2S_2): *ECONOMIC GEOLOGY*, v. 70, p. 591–594.
- Gervilla, F., Papunen, H., Kojonen, K., and Johanson, B., 1997, Results of trace element analysis of platinum-group element arsenides and sulfarsenides from some Finnish PGE-bearing mafic-ultramafic intrusions, in Papunen, H., ed., *Mineral deposits: Rotterdam, Balkema*, p. 423–426.
- Graham, J., Robinson, B.W., and Walker, R.K., 1989, Gold in arsenopyrite: *AusIMM Mineralogy-Petrology Symposium, Sydney, Proceedings*, p. 55–57.
- Johansen, B., and Kojonen, K., 1996, Results of major and trace analyses of kimberlitic garnet: *European Microbeam Analysis Society (EMAS) Regional Workshop, "Electron Probe Microanalysis Today—Practical Aspects," 2nd, Balatonfüred, Hungary, 19–22 March 1996, Proceedings*, p. 24–25.
- Karimi, M., 1992, *Geology, petrography, and mineralogical studies of Zarshuran gold deposit: Tehran, Kansaran Engineering Consultant*, 250 p. (in Persian).
- Kojonen, K., and Johansen, B., 1997, Ore microscopy and microprobe results of invisible gold in pyrite and arsenopyrite: *International Mineralogical Association-Commission on Ore Mineralogy Short Course on "Modern Approach to Ore and Environmental Mineralogy," Laboratório do IGM, S. Mamedá da Infesta, Portugal, 8–10 September, 1997*, p. 1–18.
- Radtke, A.S., 1985, *Geology of the Carlin gold deposit, Nevada: U.S. Geological Survey Professional Paper 1267*, 124 p.
- Radtke, A.S., Taylor, C., and Christ, C.L., 1972, Chemical distribution of gold and mercury at the Carlin deposit, Nevada [abs.]: *Geological Society of America Annual Meeting, Abstracts*, v. 4, p. 632.
- Robinson, B.W., and Graham, J., 1992, Advances in electron microprobe trace element analysis: *Journal of Computer-Assisted Microscopy*, v. 4, p. 263–265.
- Samimi, M., 1992, *Reconnaissance and preliminary exploration in the Zarshuran area: Tehran, Kavoshgaran Engineering Consultant*, 47 p. (in Persian).
- Wells, J.D., and Mullens, T.E., 1973, Gold-bearing arsenian pyrite determined by microprobe analysis, Cortez and Carlin gold mines, Nevada: *ECONOMIC GEOLOGY*, v. 68, p. 187–201.
- Zieboldt, T.O., 1967, Precision and sensitivity in electron microprobe analysis: *Analytical Chemistry*, v. 39, p. 858–861.